Study of crystal-field splitting in ultrathin $CePt_5$ films by Raman spectroscopy

B. Halbig,* U. Bass, and J. Geurts
Physikalisches Institut, Experimental Physics 3, Universität Würzburg, Am Hubland, D-97074 Würzburg, Germany

M. Zinner† and K. Fauth
Physikalisches Institut, Experimental Physics 2, Universität Würzburg, Am Hubland, D-97074 Würzburg, Germany
(Received 15 November 2016; revised manuscript received 10 February 2017; published 12 April 2017)

The low-temperature electronic properties of rare-earth intermetallics are substantially influenced by the symmetry and magnitude of the crystal electric field. The direct spectroscopic analysis of crystal-field splitting can be challenging, especially in low-dimensional systems, because it requires both high spectral resolution and pronounced sensitivity. We demonstrate the eligibility of electronic Raman spectroscopy for this purpose by the direct determination of the $4f$ level splitting in ultrathin ordered $CePt_5$ films down to $\approx$1.5 nm thickness on Pt(111). Crystal-field excitations of Ce $4f$ electrons give rise to Raman peaks at energy losses up to $\approx$25 meV. Three distinct peaks occur which we attribute to inequivalent Ce sites, located (i) at the interface to the substrate, (ii) next to the Pt-terminated film surface, and (iii) in the $CePt_5$ layers in between. The well-resolved Raman signatures allow us to identify a reduced crystal-field splitting at the interface and an enhancement at the surface, highlighting its strong dependence on the local atomic environment.

DOI: 10.1103/PhysRevB.95.165115

I. INTRODUCTION

In metallic systems containing $4f$ elements, the hybridization of localized $4f$ states with conduction electrons, combined with strong local Coulomb correlation, may lead to various manifestations of the fascinating field of Kondo and heavy fermion physics [1–6]. Thermodynamic and magnetic properties in these materials strongly depend on the $4f$ level splitting by the crystal electric field (CF). Its determination is thus a vital ingredient for a full appreciation of the interplay between CF splitting, orbital hybridization, and Kondo screening. However, inelastic neutron scattering (INS), well established for the determination of this splitting in bulk materials, requires large sample volumina. Therefore, the rising interest in low-dimensional correlated systems calls for complementary spectroscopic methods which are applicable to ultrathin films.

An interesting representative of the latter kind of systems is the interdiffusion-induced binary intermetallic Ce-Pt surface phase $CePt_5$ with a thickness of few unit cells on a Pt(111) substrate [7,8]. The atomic lattice of the $CePt_5$ surface film is based on the $CaCu_5$ structure, as shown in Fig. 1(a). Its symmetry is hexagonal, consisting of alternating $CePt_2$ layers and Pt layers. While the atoms in the Pt layers of the regular $CePt_5$ lattice form kagome structures, in the outermost Pt monolayer the kagome hole positions are filled, resulting in a dense hexagonal Pt-terminated surface [9,10].

The observation of Kondo screening in $CePt_5$/Pt(111) [7,11] may appear quite remarkable since bulk $CePt_5$ was reported to not exhibit Kondo interactions [12]. Valuable information on the details of the underlying mechanisms and interactions on the atomic level was obtained from intrinsically surface-specific methods, such as soft x-ray absorption (XAS) and magnetic circular dichroism (XMCD) [7,11]. It is nontrivial, however, to independently assess the crystal-field splitting and the quantitative strength of Kondo screening which both affect the magnitude and temperature dependence of the paramagnetic response [11,13]. Therefore, there is a need for an independent experimental method for the direct determination of the CF-induced Ce $4f$ level splitting in such ultrathin films with a resolution as high as possible.

In recent years, Raman spectroscopy (RS) as an optical technique, commonly used for investigating phonons in nonmetallic bulk and multilayer systems such as semiconductor heterostructures [14], has advanced to a sensitive probe for vibration eigenmodes of surfaces as well as ordered atomic overlayers [15–20]. This development was boosted by exploiting resonance enhancement of the excitation process and by the huge improvement of the detection sensitivity. Notable advantages of RS are its high spectral resolution and its ability to reveal excitation symmetry properties by utilizing well-defined light polarization configurations. Besides vibration studies, RS has also been utilized for investigating electronic excitations, including a few rare-earth CF excitation studies [21]. To our knowledge, the Raman results from $4f$ electrons published to date originate from bulk samples [22–25].

Here, we report on the direct determination of the CF-induced $4f$ level splitting in ultrathin $CePt_5$ films (between 3.5 and 18.0 unit cells) from crystal-field excitations (CEs) in *in situ* electronic Raman scattering in UHV. Three distinct CE Raman peaks are identified. Their electronic nature follows from both their temperature dependence and their absence in isostructural $LaPt_5$ films without $4f$ electrons, whereas both materials feature very similar vibrational Raman peaks. The CE peaks of $CePt_5$ exhibit individual evolutions of intensity versus $CePt_5$ film thickness. This allows us to assign them to spatially distinct Ce positions in the specimens, i.e., at the $CePt_5$/Pt(111) interface, "bulklike" sites, and those adjacent to the Pt surface termination layer.

II. EXPERIMENT

The specimens of the present study were prepared essentially according to the procedures reported in the literature [13,26,27]. In brief, clean Pt(111) surfaces were prepared by

*benedikt.halbig@physik.uni-wuerzburg.de
†martin.zinner@physik.uni-wuerzburg.de

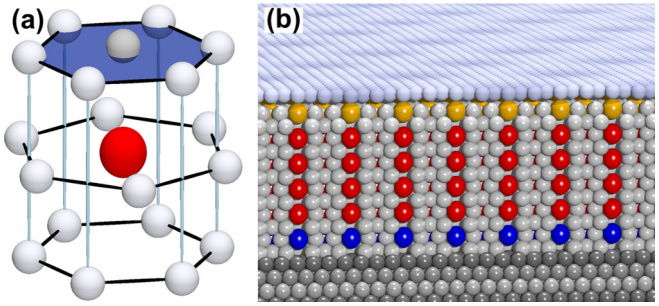

FIG. 1. $CePt_5$ lattice structure. (a) Ce atom (large red sphere) within the hexagonal elementary cell. (b) Cross section of a 6 u.c. $CePt_5$ film on Pt(111). Same color code for inequivalent Ce atoms (i.e., in proximity of the surface, the interface, or within the film) as in Figs. 3 and 4.

repeated cycles of 1 keV Ar^+ ion sputtering and annealing at $T = 1170$ K. The surface intermetallic phases were then generated by evaporating the desired amount of Ce (La) onto the substrate near ambient temperature and subsequent annealing to $T = 920$ K for 5–10 min. They are readily identified by their characteristic low-energy electron diffraction (LEED) patterns [7]. For the La-Pt system we observe a similar succession of structural phases as in $CePt_5$ [9,26] which, however, evolves much faster with coverage. From the reported evidence and similarities between the phases [27,28], Auger electron spectroscopy, and the results below, we conclude that the La-Pt phases consist of $LaPt_5$. In line with previous work, we specify the intermetallic thickness t_{nom} in nominal multiples of unit cells (u.c.) along the surface normal (1 u.c. $\approx$ 0.44 nm).

The freshly prepared specimens were transferred *in situ* into the UHV optical analysis chamber (residual pressure $p < 2 \times 10^{-10}$ mbar) and mounted onto a continuous-flow He cryostat. An initial set of Raman spectra taken at room temperature (RT) was followed by a series of low-temperature measurements (LT, $T \approx 20$ K). The samples were excited by the 2.54 and 2.41 eV lines of an Ar^+-ion laser (incident power: 100 mW), focused by a lens with focal length $f = 300$ mm.

The scattered light was collected in near-backscattering geometry by an $f/3$ lens system and analyzed by a single monochromator (SPEX 1000M) with CCD detector (ANDOR iDus series, quantum efficiency $\approx$85%). An ultrasteep long-pass edge filter (SEMROCK RazorEdge) in the optical path allowed the detection of Raman signals down to 9 meV from the laser line. The energy resolution [full width at half maximum (FWHM)] was approximately 0.4 meV. Polarization-dependent spectra were recorded with vertically polarized incident radiation and either vertically (vv) or horizontally (vh) polarized detection. Spectra taken without polarization selection will be denoted as vu. Typical integration times for a single spectrum amounted to 900 s.

III. RESULTS AND DISCUSSION

Figure 2(a) displays the RT Raman spectra for the largest thickness for both $CePt_5$ ($t_{nom} = 18$ u.c.) and $LaPt_5$ ($t_{nom} = 12$ u.c.). For both materials the vu spectra exhibit three pronounced Raman peaks between 12 and 18 meV, labeled

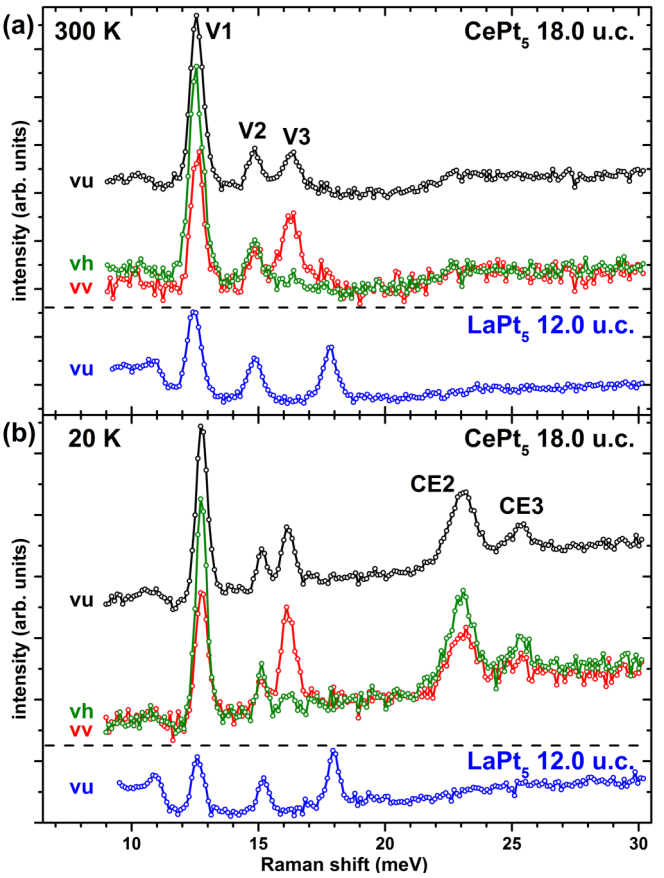

FIG. 2. (a) Raman spectra of a $CePt_5$ surface film (18 u.c.) on Pt(111), and a reference sample with a $LaPt_5$ surface film (12 u.c.), taken at $T = 300$ K. (b) Corresponding spectra at $T \approx 20$ K. vv and vh denote the polarization directions of the incoming (v) and scattered (either v or h) light; vu: unpolarized detection. Incident photon energy: 2.54 eV.

as V1, V2, and V3. They are attributed to vibration modes owing to their polarization and thickness dependence (see Fig. 3 below) as follows. Bulk $CePt_5$ and $LaPt_5$ both crystallize in the $CaCu_5$ structure ($P6/mmm$, D^1_{6h}, No. 191) [29], which exhibits only one Raman active mode, whose symmetry is E_{2g} (x^2-y^2, xy) or Γ^+_6 [30,31]. According to its Raman tensor, this bulk mode should be visible in the vv as well as the vh configuration, as is in fact observed for peak V1. This assignment is underscored by the dependence of the peak intensity on t_{nom}, as illustrated in Fig. 3. Increasing the $CePt_5$ thickness obviously entails the increase of the V1 intensity which we attribute to the growing "inner volume" of the intermetallic film. In contrast, features V2 and V3 show much less of a thickness dependence. We therefore attribute them to the uppermost region of the intermetallic film, where the lattice symmetry is reduced from D_{6h} to C_{6v} due to structural relaxations, as shown by a recent LEED-IV analysis [9]. As a result, four additional modes are now Raman allowed, two of which (E_2 and A_1) possess the polarization dependences observed for V2 and V3. These assignments are readily transferred to the $LaPt_5$ specimens, since the polarization dependence of their vibration features (not shown) matches that of $CePt_5$. At LT [Fig. 2(b)] the vibrational Raman peaks

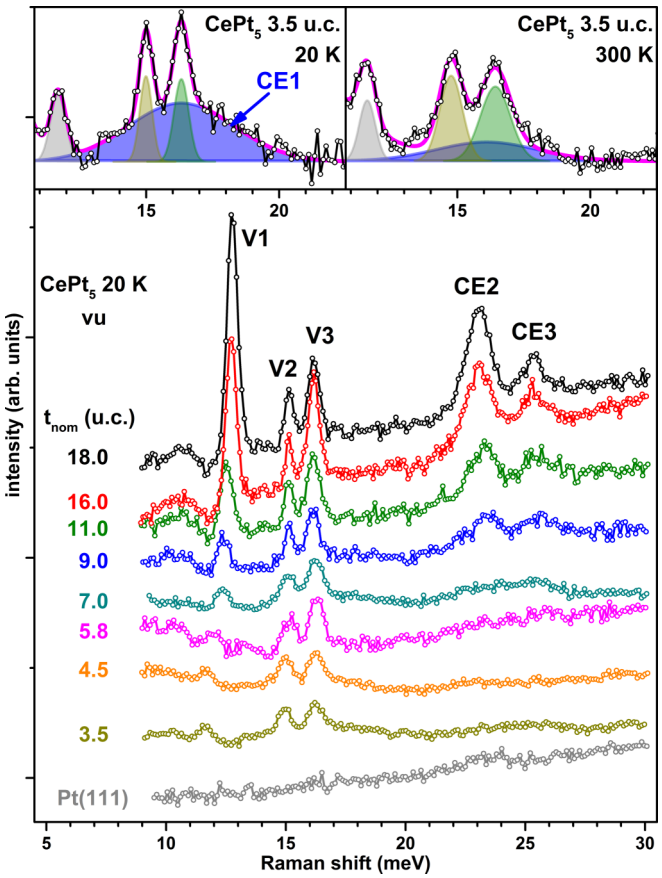

FIG. 3. Unpolarized, background-subtracted Raman spectra of the bare Pt(111) substrate and $CePt_5$ films with thickness between 3.5 and 18 u.c., taken at $T \approx 20$ K. Spectra vertically offset for clarity. Insets: Zooms into the 3.5 u.c. spectrum at 20 K (left) and 300 K (right), respectively, along with the fits of peaks V1, V2, V3, and CE1.

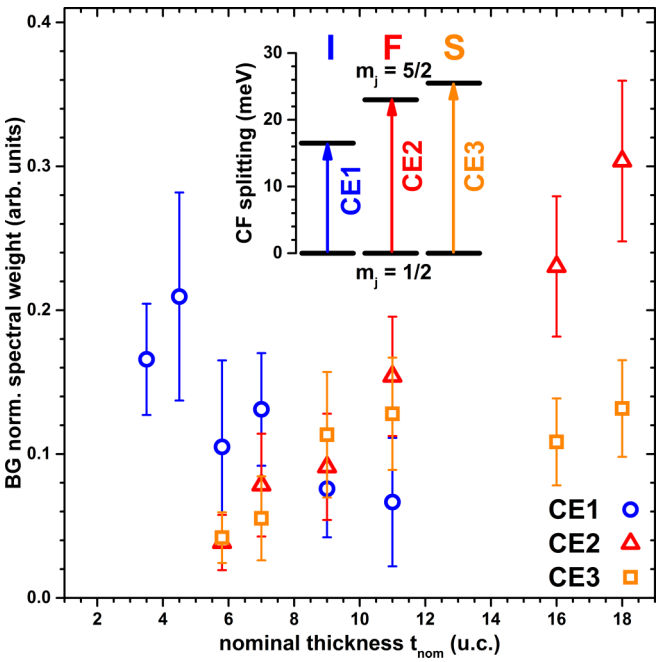

FIG. 4. $CePt_5$ film thickness dependence of the Raman intensities at $T \approx 20$ K of electronic transitions CE1 to CE3 between crystal-field-split Ce $4f$ levels. These crystal-field excitations are denoted as CE1 to CE3. Inset: Schematic assignment of the CF excitations to interface (I), film (F), and surface (S).

exhibit reduced linewidths as well as small but systematic frequency shifts, the detailed discussion of which is deferred to a later publication [32].

Here, we focus on the remarkable difference between the two materials, represented by the emergence of two new Raman peaks in $CePt_5$ for LT at loss energies of (23.1 ± 0.2) meV (CE2) and (25.4 ± 0.1) meV (CE3), while obviously absent in $LaPt_5$ [Fig. 2(b)]. In hindsight, a faint contribution of these features may already be discerned in the RT spectra. A third peak will be identified below. No other spectral signatures were found up to 180 meV.

We attribute the additional Raman peaks in the $CePt_5$ spectrum to Ce $4f$ CF excitations. This seems to be a natural choice since the main difference of Ce with respect to La consists of the extra $4f$ electron, and CF excitations generally acquire more intensity at low temperature [21]. The appropriateness of this attribution may once again be discussed based on the polarization dependence of the new features, which is similar to that of V1. In the CF picture the hexagonal symmetry of the Ce site in $CePt_5$ leads to a splitting of the $j = \frac{5}{2}$ multiplet into three Kramers doublets of pure $m_j = \pm\frac{1}{2}, \pm\frac{3}{2}$, and $\pm\frac{5}{2}$ character, which belong to the double group representations Γ_7^-, Γ_9^-, and Γ_8^-, respectively [21,33]. Since the quadrupole selection rules for CE Raman transitions in the present geometry require $\Delta m_j = \pm 2$, only the transitions involving the $m_j = \pm\frac{1}{2}$ doublet are symmetry allowed, i.e., $\Gamma_7^- \leftrightarrow \Gamma_9^-$ $(\pm\frac{1}{2} \leftrightarrow \mp\frac{3}{2})$ and $\Gamma_7^- \leftrightarrow \Gamma_8^-$ $(\pm\frac{1}{2} \leftrightarrow \pm\frac{5}{2})$. Their polarization dependence is encoded in the irreducible representations contained in the direct products $\Gamma_7^- \otimes \Gamma_9^-$ and $\Gamma_7^- \otimes \Gamma_8^-$, respectively. Both share Γ_6^+ as a member, which we already identified with the vibration mode V1. The symmetry analysis thus leads us to expect that the CE peaks and V1 have the same polarization dependence, which is readily confirmed for CE2 and CE3 from Fig. 2(b). A closer inspection of the $CePt_5$ LT Raman spectra at small t_{nom} reveals that there is actually a third, significantly broader excitation, as shown in the left inset to Fig. 3. With an energy of (16.4 ± 0.5) meV and FWHM of $\approx$4 meV it energetically overlaps with the vibration peaks V2 and V3, but is indispensable for an accurate fit. At RT, it appears only allusively, as shown in the right inset. Moreover, it is absent in $LaPt_5$ [31]. Therefore, this feature is again associated with a CF excitation and labeled as CE1.

The observation of three distinct CE excitations clearly cannot be reconciled with a single CF splitting scheme valid for all Ce sites alike. The key to their understanding lies in evaluating their intensities as a function of intermetallic film thickness t_{nom}. To this end, each Raman spectrum was subjected to a least squares fit by a superposition of Gaussians above a linear background [31]. In Fig. 4, we report the intensities of the LT electronic Raman peaks, normalized to the electronic background intensity around 20 meV, where no contribution to any peak occurs at any t_{nom}. This normalization compensates for possible spectrum-to-spectrum intensity variations due to different focusing and optical align-

ments. The intensity dependence on t_{nom} is quite individual: While CE1 rapidly decreases with increasing film thickness and vanishes for $t_{\mathrm{nom}} \gtrsim 10$ u.c., in contrast, CE2 shows a complementary increase, and CE3 is thickness independent within experimental error for $t_{\mathrm{nom}} \gtrsim 7$ u.c. Therefore we assign the different CF excitations to Ce atoms with different local environments in the intermetallic films.

The rapid decrease of the CE1 intensity suggests that it is related to the Ce sites in the vicinity of the interface to the Pt(111) substrate. Its rate of decay with t_{nom} leads to an estimated attenuation length of $\lambda \approx (6.0 \pm 1.5)$ nm. The steady growth of the CE2 intensity is very reminiscent of the behavior of the vibration peak V1 of the $CePt_5$ film and hence suggestive of associating it with the CF excitations in the "inner," bulklike volume of the film. Based on the λ estimate, however, one would expect a signature of saturating intensity of CE2 as well as V1 in the limit of largest t_{nom}, which is clearly not the case. A nonsaturating growth of V1 may arise from an increase of scattering efficiency upon gradually acquiring bulklike symmetry with increasing film thickness. This will also lead to stronger electronic scattering provided there is significant coupling to the vibration mode. Such coupling was indeed discussed and detected in earlier work [22,34,35]. Finally, the nearly thickness-independent intensity of feature CE3 points to CF excitations limited to the vicinity of the film surface. The spatial dependence of the CF energies highlights that the CF splitting may sensitively depend on the local surroundings "even in a metal." A similar conclusion was recently reached concerning the nature of the electronic ground state in a Ce-Pd surface alloy, based on photoemission results [36].

A conclusion with respect to the character of the CE transitions ($\Gamma_7^- \leftrightarrow \Gamma_9^-$ vs $\Gamma_7^- \leftrightarrow \Gamma_8^-$) can be reached by using complementary information. From XAS experiments it was concluded that the states with $m_j = \pm\frac{5}{2}$ are highest in energy and that the splitting between the states with $m_j = \pm\frac{1}{2}$ and $m_j = \pm\frac{3}{2}$ amounts to less than 1 meV [11,37]. On this basis we can unanimously state that the Raman losses observed here all are of $\Gamma_7^- \leftrightarrow \Gamma_8^-$ character and represent excitations from lower-lying states with $m_j = \pm\frac{1}{2}$ to excited states with $m_j = \pm\frac{5}{2}$. The temperature dependence of x-ray linear and circular dichroism at the Ce $M_{4,5}$ edges furthermore suggested an energy scale for the total CF level spread of $\lesssim$18 meV for $t_{\mathrm{nom}} \lesssim 4$ u.c. and $\gtrsim$25 meV for $t_{\mathrm{nom}} \gtrsim 7$ u.c. Given that the XAS probing depth is smaller by roughly a factor of 4–6 compared to the present work, this level of almost quantitative agreement is extremely gratifying. Both sets of experiments also agree in that no higher lying CF excitations are observed in the ultrathin $CePt_5$ films. Detecting the CF excitations by Raman scattering offers the compelling advantage of high spectral resolution, though. It allows us to discriminate between coexisting Ce $4f$ schemes involving minute differences at the quantitative level which would otherwise go unnoticed. Also, the level of accuracy achievable by direct observation of the excitations exceeds by far the potential of fitting Boltzmann distributions in temperature-dependent experiments.

The high spectral resolution also allows one to examine the CE peaks widths and especially to address the question of the broadening of CE1 compared to CE2 and CE3. Here, we can draw an analogy with INS on bulk samples. Recently, Willers *et al.* [38] have noted for Ce compounds a positive correlation between the width of CF excitations in INS and the hybridization strength between Ce $4f$ electrons and itinerant states seen by XAS, suggesting that hybridization contributes significantly to reducing the lifetime of the CF excited states. In this respect our Raman results are fully in line with these INS observations. The CE1 excitation relates to the CF splitting scheme which is predominant at small film thickness and is characterized by a large Raman peak width. This is also the thickness regime of strongest Ce $4f$ hybridization [7]. Interestingly, the regime of stronger hybridization and hence stronger Kondo screening [7,11] correlates with the occurrence of a smaller overall CF splitting. A similar conclusion seems to hold in the case of $CeAg_x$ films, albeit on a strongly reduced energy scale [39].

IV. SUMMARY

In summary, we have shown that, besides the vibration modes, also the CF splitting of $4f$ electron levels can be determined directly with high accuracy by Raman scattering from electronic transitions between CF-split levels, even for ultrathin intermetallic films comprising just a few atomic layers and a moderate density of rare-earth atoms. In our exemplary study of $CePt_5$/Pt(111), the observation of three distinct CE Raman peaks from Ce atoms at the $CePt_5$-Pt(111) interface, within "bulklike" $CePt_5$ layers, and adjacent to the film surface, reveals the different crystal fields of these atomic environments. The small energy difference between CE2 and CE3 in particular could hardly have been resolved by other means. The electronic origin of these Raman peaks is substantiated by their absence in isostructural $LaPt_5$, and their polarization dependence is in accordance with the lattice symmetry. Raman spectroscopy thus lends itself as a viable laboratory-scale alternative for analyzing the crystal-field level structure of ultrathin metallic rare-earth compounds with high sensitivity and accuracy.

ACKNOWLEDGMENTS

We gratefully acknowledge financial support by the Deutsche Forschungsgemeinschaft through the research unit FOR 1162 (Projects No. Ge1855/10-2 and Fa222/5-2) as well as experimental support by R. Hölldobler.

B.H. and M.Z. contributed equally to this work.

[1] A. C. Hewson, *The Kondo Problem to Heavy Fermions* (Cambridge University Press, Cambridge, U.K., 1993).

[2] N. Grewe and F. Steglich, in *Handbook on the Physics and Chemistry of Rare Earths*, edited by K. A. Gschneider, Jr. and L. Eyring (Elsevier, Amsterdam, 1991), Vol. 14, p. 343.

[3] H. v. Löhneysen, A. Rosch, M. Vojta, and P. Wölfle, Rev. Mod. Phys. **79**, 1015 (2007).
[4] Y.-F. Yang, Rep. Prog. Phys. **79**, 074501 (2016).
[5] F. Steglich and S. Wirth, Rep. Prog. Phys. **79**, 084502 (2016).
[6] D. Pines, Rep. Prog. Phys. **79**, 092501 (2016).
[7] C. Praetorius, M. Zinner, A. Köhl, H. Kießling, S. Brück, B. Muenzing, M. Kamp, T. Kachel, F. Choueikani, P. Ohresser *et al.*, Phys. Rev. B **92**, 045116 (2015).
[8] M. Klein, A. Nuber, H. Schwab, C. Albers, N. Tobita, M. Higashiguchi, J. Jiang, S. Fukuda, K. Tanaka, K. Shimada *et al.*, Phys. Rev. Lett. **106**, 186407 (2011).
[9] C. Praetorius, M. Zinner, G. Held, and K. Fauth, Phys. Rev. B **92**, 195427 (2015).
[10] P. Tereshchuk, M. J. Piotrowski, and J. L. F. Da Silva, RSC Adv. **5**, 521 (2015).
[11] C. Praetorius and K. Fauth, Phys. Rev. B **95**, 115113 (2017).
[12] H. Lueken, M. Meier, G. Klessen, W. Bronger, and J. Fleischhauer, J. Less-Common Met. **63**, 35 (1979).
[13] C. Praetorius, M. Zinner, P. Hansmann, M. W. Haverkort, and K. Fauth, Phys. Rev. B **93**, 165107 (2016).
[14] J. Geurts, Prog. Cryst. Growth Charact. Mater. **32**, 185 (1996).
[15] N. Esser, Appl. Phys. A **69**, 507 (1999).
[16] N. Esser and W. Richter, in *Light Scattering in Solids VIII: Fullerenes, Semiconductor Surfaces, Coherent Phonons*, edited by M. Cardona and G. Güntherodt (Springer, Berlin, 2000), Vol. 76, pp. 96–168.
[17] J. Räthel, E. Speiser, N. Esser, U. Bass, S. Meyer, J. Schäfer, and J. Geurts, Phys. Rev. B **86**, 035312 (2012).
[18] V. Wagner, J. Wagner, S. Gundel, L. Hansen, and J. Geurts, Phys. Rev. Lett. **89**, 166103 (2002).
[19] M. Liebhaber, U. Bass, P. Bayersdorfer, J. Geurts, E. Speiser, J. Räthel, A. Baumann, S. Chandola, and N. Esser, Phys. Rev. B **89**, 045313 (2014).
[20] M. Liebhaber, B. Halbig, U. Bass, J. Geurts, S. Neufeld, S. Sanna, W. G. Schmidt, E. Speiser, J. Räthel, S. Chandola, and N. Esser, Phys. Rev. B **94**, 235304 (2016).
[21] G. Schaack, in *Light Scattering in Solids VII: Crystal-Field and Magnetic Excitations*, edited by M. Cardona and G. Güntherodt (Springer, Berlin, 2000), Vol. 75, pp. 24–173.
[22] G. Güntherodt, A. Jayaraman, B. Batlogg, M. Croft, and E. Melczer, Phys. Rev. Lett. **51**, 2330 (1983).
[23] E. Zirngiebl, B. Hillebrands, S. Blumenröder, G. Güntherodt, M. Loewenhaupt, J. M. Carpenter, K. Winzer, and Z. Fisk, Phys. Rev. B **30**, 4052 (1984).
[24] G. Güntherodt, E. Zirngiebl, S. Blumenröder, A. Jayaraman, B. Batlogg, M. Croft, and E. Melczer, J. Magn. Magn. Mater. **47**, 315 (1985).
[25] S. L. Cooper, M. V. Klein, Z. Fisk, and J. L. Smith, Phys. Rev. B **34**, 6235 (1986).
[26] J. Kemmer, C. Praetorius, A. Krönlein, P.-J. Hsu, K. Fauth, and M. Bode, Phys. Rev. B **90**, 195401 (2014).
[27] M. Garnier, D. Purdie, K. Breuer, M. Hengsberger, and Y. Baer, Phys. Rev. B **58**, 9697 (1998).
[28] A. Ramstad, S. Raaen, and N. Barrett, Surf. Sci. **448**, 179 (2000).
[29] B. Predel, in *The Landolt-Börnstein Database*, edited by O. Madelung (Springer, Berlin, 1993), Vol. 5c.
[30] D. L. Rousseau, R. P. Bauman, and S. P. S. Porto, J. Raman Spectrosc. **10**, 253 (1981).
[31] See Supplemental Material at http://link.aps.org/supplemental/10.1103/PhysRevB.95.165115 for a group theoretical analysis, the identification of CE1 by a comparison of $CePt_5$ and $LaPt_5$, and fits of Raman spectra over a wide spectral range.
[32] B. Halbig *et al.* (unpublished).
[33] A. Kiel and S. Porto, J. Mol. Spectrosc. **32**, 458 (1969).
[34] M. Loewenhaupt, U. Witte, S. Kramp, M. Braden, and P. Svoboda, Physica B **312-313**, 181 (2002).
[35] R. Schedler, U. Witte, M. Loewenhaupt, and J. Kulda, Physica B **335**, 41 (2003).
[36] M. Mulazzi, K. Shimada, J. Jiang, H. Iwasawa, and F. Reinert, Phys. Rev. B **89**, 205134 (2014).
[37] C. Praetorius, Ce $M_{4,5}$ XAS and XMCD as local probes for Kondo and heavy fermion materials: A study of $CePt_5$/Pt(111) surface intermetallics, Ph.D. thesis, University Würzburg, 2015.
[38] T. Willers, Z. Hu, N. Hollmann, P. O. Korner, J. Gegner, T. Burnus, H. Fujiwara, A. Tanaka, D. Schmitz, H. H. Hsieh *et al.*, Phys. Rev. B **81**, 195114 (2010).
[39] M. Zinner *et al.* (unpublished).